Analysis of Doubly-Fed Induction Generator Driven by Wind Turbine Using Real Time Digital Simulator

Satish Choudhury, Kanungo Barada Mohanty

Department of Electrical Engineering
National Institute of Technology
choudhury.satish@yahoo.com

Abstract-**Doubly-fed Induction Generator (DFIG) is the most common rotatory machine which is used on the grid connected wind energy conversion system for the fulfillment of the system requirement such as grid stability, fault ride through (FRT), power quality improvement, and grid synchronization and power control etc. Though the requirements are not fulfilled directly by the machine rather the control strategy is used in both the stator as well as rotor side along with converters to fulfill the requirements stated above. To satisfy the grid code requirements of wind turbine, usually grid side converter is playing a major role. So in order to improve the operation capacity of wind turbine under critical situation, the intensive study of both machine side converter control and grid side converter control is necessary. The machine uses two back-to-back converters. The grid side converter is modeled to control the active and reactive power independently along with dc-link voltage. The machine side converter is modeled to control the reactive power of the machine and maintain the speed constant irrespective of the transient behavior of the grid. In this paper the performance of the DFIG system is analyzed under grid voltage fluctuation and the theoretical results are obtained from the MATLAB/ SIMULINK environment. The proposed work is also validated experimentally using RT-LAB.**

Keyword-Doubly-fed Induction Generator (DFIG); Vector control; PWM Converter; Grid-side converter; Machine-side converter; RT-LAB

I.   INTRODUCTION

The motion of air masses due to different thermal conditions causes wind to flow is a most common local or global phenomenon but the versatility nature of wind led to pollution free electricity generation which was first developed at the beginning of the twentieth century. The technology was stepped up in a techno stare case from early seventies to achieve the successive steps. By the end of nineties wind energy achieve its goal as one of the most important sustainable energy resources. The importance of these sources highlights some of the basic requirements such as turbine, generators etc. To satisfy basic needs the realization of above requirements is necessary.

In this paper the requirement of generator is being filled by DFIG system. The focus is made on the performance characteristics of DFIG under grid voltage fluctuation. The control strategy is made to satisfy grid codes such as grid stability, fault ride through (FRT), power quality improvement, grid synchronization and power control etc. DFIG system uses back-to-back converters in the rotor circuits to meet the necessary requirements. Out of two converters grid side converter satisfies the grid codes [1] and the machine side converter satisfies the machine codes. The doubly fed induction machine using an AC-AC converter in the rotor circuit (Scherbius drive) has long been a standard drive option for high-power applications involving a limited speed range. The power converter need only be rated to handle the rotor power [2]. A current fed inverter controlled DFIG with a variable rotor side frequency is well explained for energy recovery in [3]. The disadvantages of energy recovery scheme of [3] are discussed in [4].

Focusing towards the grid side converter the following analysis has been made from the different literatures. Independent control of active and reactive power from the grid or to the grid is possible by vector control of line side converter [5]. The traditional voltage oriented control (VOC) of grid side converter has been studied under balanced condition of the 3-Φ grid in [6]. Different control techniques are used in the literatures to improve FRT capability of DFIG system. Such system uses a robust linear quadratic LQ controller is synthesized to improve the FRT capability as well as the generator performance under grid voltage unbalance [7], a series converter on the stator terminal is used to mitigate the effect of the short circuit on the wind turbine [8], a controller is proposed which uses the positive and negative sequence component to work under FRT [9]. During unbalanced conditions of the 3-Φ grid voltages, operation of grid side converter is critical due to failure of detecting exact stator flux position for voltage oriented control algorithm. For that VOC-RRF control strategy is proposed in [10] without using flux position estimation. But, it has been shown that both even harmonics and odd harmonics appear in dc link voltage and ac side input currents respectively during unbalanced 3-Φ grid voltages [11].

In this paper traditional voltage control technique is used in both grid-side as well as machine-side converters to analyze the performance of the DFIG system under grid voltage fluctuation and the theoretical results are obtained from the MATLAB/ SIMULINK environment. The results are also verified experimentally using RTDS where RT-LAB is used. In RT-LAB hardware synchronization mode is selected to synchronize the software environment with the hardware environment via an analog peripheral OP5251.

II.   MODELING OF DFIG

A 10 h.p. wound rotor induction machine is modeled in synchronous reference frame. The schematic diagram of the overall system is shown in Fig.1. Two voltage fed PWM converters are used in the model, one is used in the grid side and other is in the machine side. The objective of grid side

converter is to maintain dc-link voltage constant and the machine side converter control regulates the speed of the prime mover thus making the system suitable for variable speed application system.
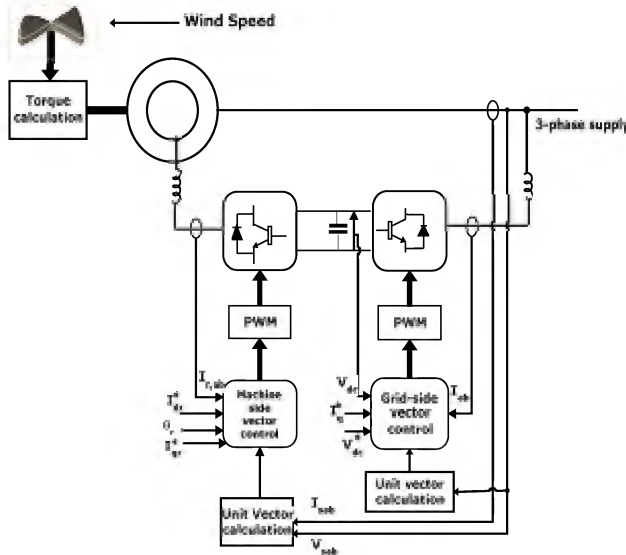

Figure 1. Overall DFIG system

Equations (1)-(4) and (8)-(9) describe the complete machine model in state-space form where Ψ_{qs}, Ψ_{ds}, Ψ_{qr}, Ψ_{dr} are the state variables. The machine is simulated using MATLAB/SIMULINK.

$$\frac{d\Psi_{qs}}{dt} = \omega_b \left[v_{qs} - \frac{\omega_e}{\omega_b} \Psi_{ds} - \frac{R_s}{X_{ls}} (\Psi_{qs} - \Psi_{qm}) \right] \qquad (1)$$

$$\frac{d\Psi_{ds}}{dt} = \omega_b \left[v_{ds} + \frac{\omega_e}{\omega_b} \Psi_{qs} - \frac{R_s}{X_{ls}} (\Psi_{ds} - \Psi_{dm}) \right] \qquad (2)$$

$$\frac{d\Psi_{qr}}{dt} = \omega_b \left[v_{qr} - \frac{R_r}{X_{lr}} (\Psi_{qr} - \Psi_{qm}) - \left(\frac{\omega_e - \omega_r}{\omega_b} \right) \Psi_{dr} \right] \qquad (3)$$

$$\frac{d\Psi_{dr}}{dt} = \omega_b \left[v_{dr} - \frac{R_r}{X_{lr}} (\Psi_{dr} - \Psi_{dm}) + \left(\frac{\omega_e - \omega_r}{\omega_b} \right) \Psi_{qr} \right] \qquad (4)$$

Where $\quad \Psi_{qm} = \dfrac{X_{ml}}{X_{ls}} \Psi_{qs} + \dfrac{X_{ml}}{X_{lr}} \Psi_{qr} \qquad (5)$

$$\Psi_{dm} = \frac{X_{ml}}{X_{ls}} \Psi_{ds} + \frac{X_{ml}}{X_{lr}} \Psi_{dr} \qquad (6)$$

$$X_{ml} = \frac{X_m X_{ls} X_{lr}}{X_{ls} X_{lr} + X_m X_{lr} + X_m X_{ls}} \qquad (7)$$

The development of torque by the interaction of airgap flux and rotor mmf can be expressed in more general form relating the d-q component of variables. The expression for the electromagnetic torque developed is given in (8).

$$T_e = \frac{3}{2} \left(\frac{p}{2} \right) \frac{1}{\omega_b} \left(\Psi_{ds} i_{qs} - \Psi_{qs} i_{ds} \right) \qquad (8)$$

The speed ω_r in the above equations cannot be treated as constant. It can be related to the torque as

$$T_e = T_m + J \frac{d\omega_m}{dt} = T_m + \frac{2}{p} J \frac{d\omega_r}{dt} \qquad (9)$$

III. GRID SIDE CONVERTER CONTROL

When the voltage in the utility grid changes abruptly due to sudden load changes and abrupt wind speed variations, it makes an effect on the machine, as a result the system voltages available across stator as well as rotor changes. Since the converters are connected back-to-back the same effect is also observed across these two converters and on the dc-link capacitor as well.

The necessary control action is adopted to maintain the dc-link voltage constant. Grid voltage oriented vector control is approached, in which the real axis of the grid voltage vector is chosen as the d-axis. Phase Locked Loop block is used to measure the system frequency and provides the phase synchronous angle θ for the d-q transformations block. The control scheme utilizes current control loops for id and iq with the id demand being derived from the dc-link voltage error through a standard PI controller. The iq demand determines the displacement factor on the grid side of the choke. The active power and reactive power is controlled independently using d-q component of the current governed by (10) and (11). The detail control strategy is shown in Fig.2.

$$P = \frac{3}{2} (v_d i_d + v_q i_q) \qquad (10)$$

$$Q = \frac{3}{2} (v_d i_q - v_q i_d) \qquad (11)$$

The reference voltage vectors for the grid side converters are found from (12) and (13).

$$v_d^* = v_d + i_q^* \omega_e L - i_d^* R - v'_d \qquad (12)$$

$$v_q^* = v_q - i_d^* \omega_e L - i_q^* R - v'_q \qquad (13)$$

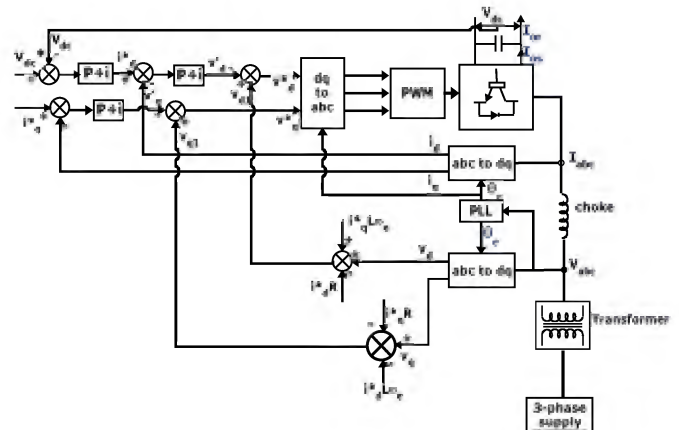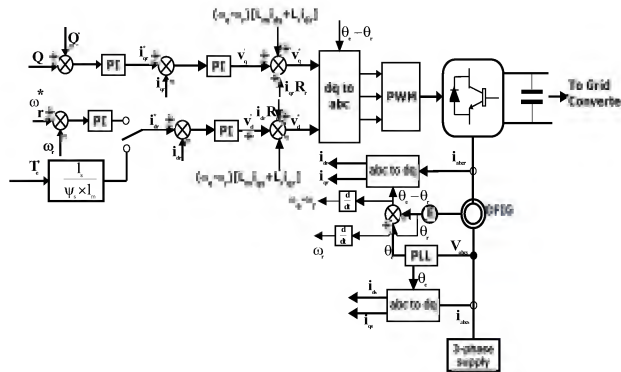Where the v'd and v'q is found from the current errors through standard PI controllers.

Figure 2. Vector control structure for grid side converter

IV. MACHINE SIDE CONVERTER CONTROL

The necessary control action is adopted for the machine side converter to maintain the speed of the DFIG constant and also control the reactive power flow from the utility grid to the machine irrespective of the wind speed.

The unit vector requirement for the d-q transformation is found by using grid voltage orientation where the real axis of the grid voltage vector is chosen as the d-axis as used in case of grid side converter control. The detail control strategy for machine side converter control is shown in Fig.3.

Figure 3.   Vector control structure for machine side converter

The reference voltage vectors for machine side converter are being derived using (14) and (15).

$$v_d^* = v_d' + i_{dr}R_r - (\omega - \omega_r)\left[i_{qr}L_r + L_m i_{qs}\right] \tag{14}$$

$$v_q^* = v_q' + i_{qr}R_r + (\omega - \omega_r)\left[i_{dr}L_r + L_m i_{ds}\right] \tag{15}$$

Where v'd and v'q is found from the current errors through standard PI controllers. The reference current i*dr can be found either from the reference torque given by (16) or form the speed errors through standard PI controllers. Similarly i*qr is found from the reactive power errors. The reactive power and speed is controlled using the current control loops.

$$i_{dr}^* = \frac{T_e^* \times L_s}{\psi_s \times L_m} \tag{16}$$

$$T_e^* = \frac{P_{mech} - P_{loss}}{\omega_r}$$

Where

$$P_{loss} = MechanicalLosses + ElectricalLosses(P_{Cur} + P_{Cus})$$

The maximum mechanical power given by (17) can be extracted from the wind is proportional to the cube of the rotor speed.

$$P_{max} = K_{opt}\,\omega^3 \tag{17}$$

Where

$$K_{opt} = \frac{1}{2}\rho C_{p,opt}\pi \frac{R^5}{\lambda_{opt}^3}$$

The optimum value of K is found from the typical power versus speed characteristics of a wind turbine. The wind turbine power curves shown in Fig.4 illustrate how the mechanical power that can be extracted from the wind depends on the rotor speed. For each wind speed there is an optimum turbine speed at which the extracted wind power at the shaft reaches its maximum.

Figure 4.   Typical power versus speed characteristics of a wind turbine

V.   SIMULATION RESULTS AND DISCUSSION

The 10hp machine is simulated with MATLAB/SIMULINK environment by taking different cases into account.

A.   Simulation under Voltage Sag

The simulation results under the voltage sag are shown in Fig.5. The DFIG system produces active power of 7 kW which corresponds to maximum mechanical turbine output minus electrical losses in generator. When the grid voltage changes suddenly from its rated value i.e.415V the stator current as well as rotor current increases and the active power P suddenly oscillates and then it settles to its rated value. The reference reactive power is set at 0KVAr but when voltage decreases the reactive power suddenly increases then it settles to 0KVAr as per the control strategy made in the rotor side converter. The dc link voltage is set at 850V by the grid side converter but at the time of voltage sag it oscillates and finally settles to its set value and the rotor speed is also maintained constant to its rated (1080rpm) while the wind speed is kept constant at 10m/s. The rotor output is same as the converter output. In Fig.5 the behavior of Vabc, Iabc, P, Q, Vdc, ωr, Vabcr, Iabcr is observed at 0.2s when the voltage decreases to 50%.

It has also been shown that the rotor flux reduces when the grid voltage suddenly decreases to 50% obeying the principle voltage is proportional to the flux. The flux path is shown in Fig.6.

B.   Simulation under Voltage Swell

It has also been shown that the rotor flux increases when the grid voltage suddenly increases to 120% obeying the principle voltage is proportional to the flux. The flux path is shown in Fig.7.
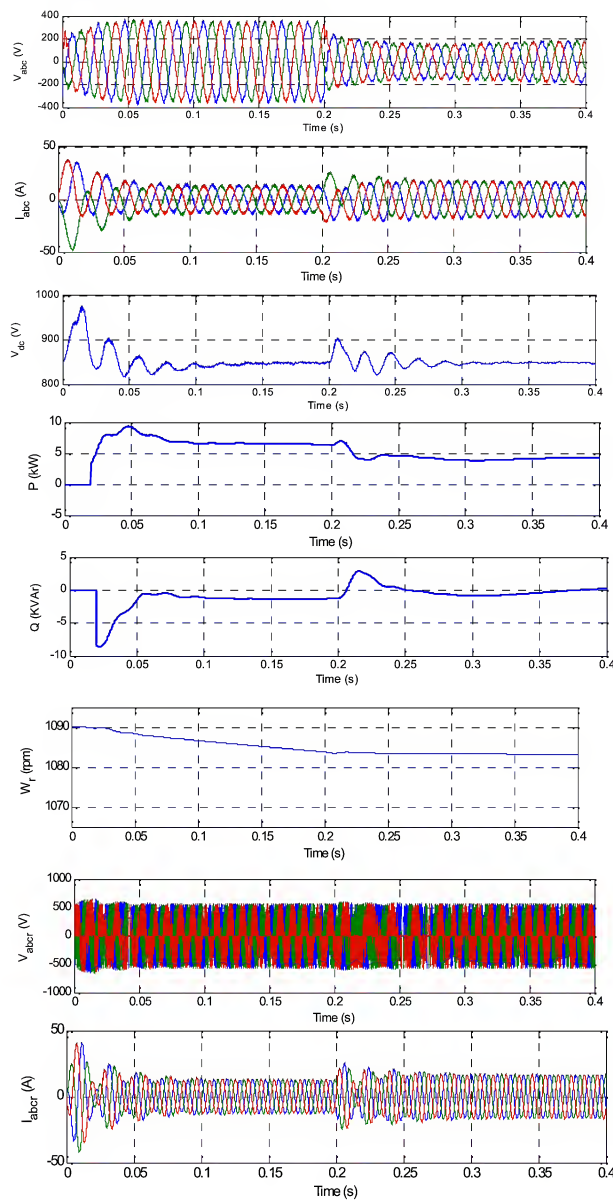
Figure 7.   Simulation results under wind speed variation
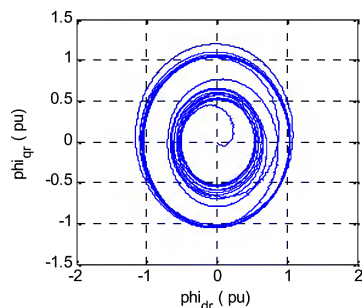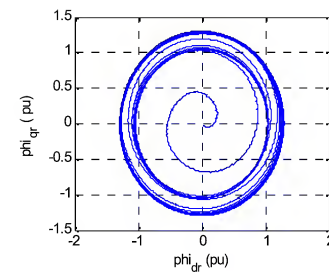
Simulation results under voltage swell is also shown in Fig.8. When the grid voltage increases up to 120% of its rated value the stator current as well as rotor current decreases and the reactive power Q decreases suddenly and then settles to 0KVAr. In Fig.7 the behavior of the generator is observed at 0.2s when the voltage rises to 120% of its rated value.

VI.   EXPERIMENTAL RESULTS

The results are also verified experimentally using RTDS where RT-LAB is used. In RT-LAB hardware synchronization mode is selected to synchronize the software environment with the hardware environment via an analog peripheral OP5251.

Figure 5.   Simulation Results Under Voltage Sag

Figure 6.   Flux path under voltage sag
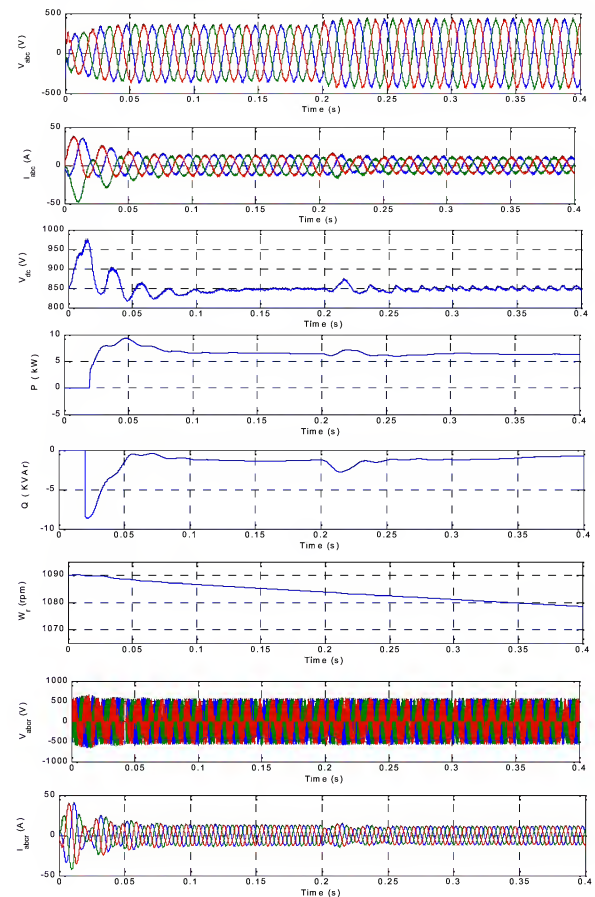
Figure 8.   Experimental results under voltage sag

increased to 150% to shows the significant changes in the parameters.
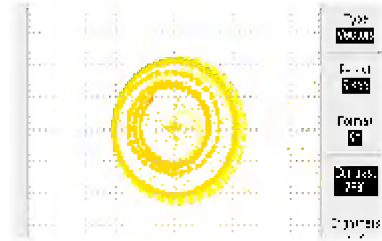
Figure 10.   Flux path under voltage sag

Figure 9.   Experimental results under voltage sag

Fig.9 shows the experimental results of V_{abc}, I_{abc}, V_{dc}, P, Q, ωr, V_{abcr}, I_{abcr} when the voltage decreases to 50%. The simulation results shown in Fig.5 are verified in Fig.9. The flux path shown in Fig.6 is also verified in Fig.10 experimentally.

Fig.11 & 12 shows the experimental verification of results of Vabc, Iabc, Vdc, P, Q, ωr, Vabcr, Iabcr shown in Fig.8 & 7 respectively under voltage swell. In this case the voltage is
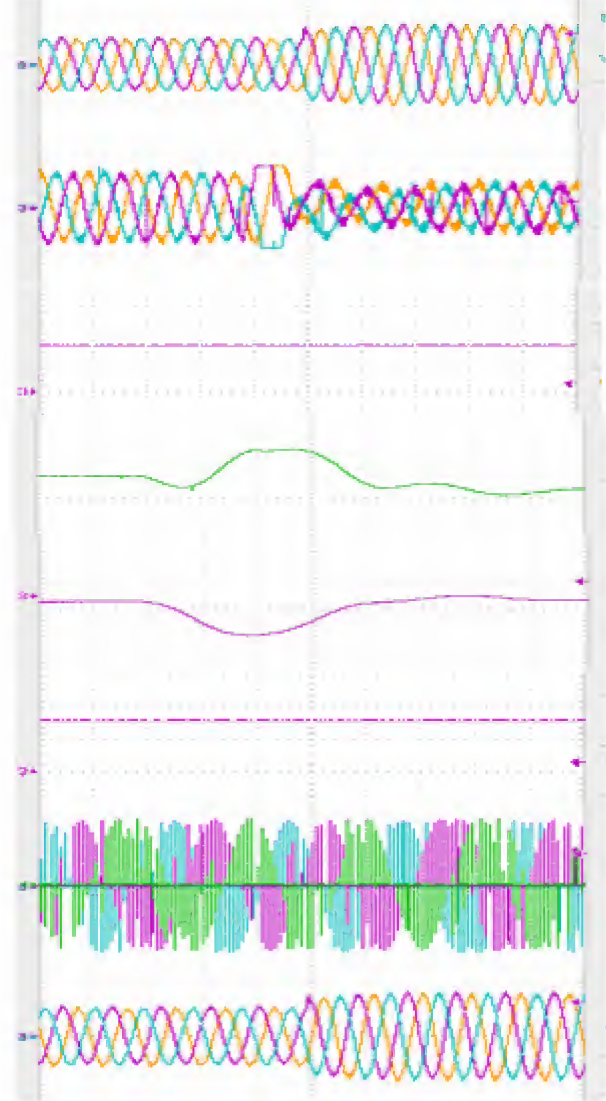

Figure 11. .Experimental results under voltage swell

VII.   CONCLUSION

A   DFIG system with a back-to-back converter is simulated using standard PI controllers. It is concluded that traditional voltage control technique which is used in both grid-side as well as machine-side converters to analyze the

performance of the DFIG system under grid voltage fluctuation is suitable under sudden change in grid voltage. The system is also verified experimentally using RTDS.
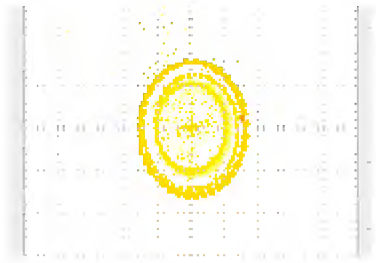

Figure 12. .Flux path under voltage swell

APPENDIX

Rated Power	10hp
Stator Voltage	415V
R$_s$(Stator Resistance)	1.11Ω
R$_r$(Rotor Resistance)	0.9Ω
L$_s$ (Stator Inductance)	0.3H
L$_m$(Mutual inductance)	0.08H(Referred to the rotor)
L$_r$ (Rotor inductance)	0.09H(Referred to the rotor)
Poles	6
Rated speed	1100 rpm
DC link Voltage	850V
Switching Frequency of IGBTs	3kHz
Dc link capacitor	10000μF

REFERENCES

[1] F. Blaabjerg, R. Teodorescu, M. Liserre and A.V. Timbus, "Overview of Control and Grid Synchronization for Distributed Power Generation Systems" IEEE Transactions on Industrial Electronics, Vol.:53, Issue: 5, 2006, pp.1398-1409.

[2] R. Pena, J. C. Clare, and G. M. Asher, "Doubly fed induction generator using back-to-back PWM converters and its application to variable-speed wind-energy generation," IEE Proc. Elect. Power Appl., May 1996, Vol. 143, No. 3, pp. 231-241.

[3] G. A. Smith, K. Nigim, and A. Smith, "Wind-energy recovery by a static Scherbius induction generator", IEE Proc. C, 1981, 128, (6), pp. 317-324.

[4] I. Cardici, and M. Ermis, "Double-output induction generator operating at sub synchronous and super synchronous speed steady state performance optimization and wind-energy recovery", IEE proc. B, 1992, 139, (5), pp. 429-442.

[5] S. R. Jones, and R. Jones, "Control strategy for sinusoidal supply side convertors", IEE Colloquium on Developments in real time control for induction motor drives, February 1993, Digest 1993/024.

[6] R. Wu, S. B. Dewan and G. R. Slemon, "Analysis of an ac to dc voltage source converter using PWM with phase and amplitude control". IEEE Trans Ind. Vol. 27, No. 2, pp. 355-364, 1991.

[7] O. S. Ebrahim , P.K. Jain, and G. Nishith, "New Control Scheme for the Wind-Driven Doubly Fed Induction Generator under Normal and Abnormal Grid Voltage Conditions" Journal of Power Electronics, Vol. 8, No. 1, January 2008, pp.10-22.

[8] O. Abdel-Baqi and A. Nasiri, "A Dynamic LVRT Solution for Doubly-Fed Induction Generators" IEEE Transactions on Power Electronics,Vol:25, Issue: 1, 2010,pp.193-196.

[9] Y. Zhou, P. Bauer, J.A. Ferreira, and J. Pierik, "Operation of Grid-Connected DFIG Under Unbalanced Grid Voltage Condition" IEEE Transactions on Energy Conversion, Vol. 24, Issue: 1, 2009,pp.240-246.

[10] P. Rodriguez, A. Luna, R. Teodorescu, F.Iov, and F. Blaabjerg, "Fault ride-through capability implementation in wind turbine converters using a decoupled double synchronous reference frame PLL". Proc. of European Conference on Power Electronics and Applications, 2007.

[11] P. N. Enjeti and S. A. Choudhury, "A new control strategy to improve the performance of a PWM AC to DC converter under unbalanced operating conditions," IEEE Trans. Power Electron., Vol. 8, No. 4, pp. 493–500, Oct. 1993.

[12] B. K. Bose "Modern Power Electronics and AC Drives" by Prentice-Hall , Inc, Publication 2002,pp.70-74.